LAUR 94-3297

TITLE: Derivation of the Weibull distribution based on physical principles and its connection to the Rossin-Rammler and lognormal distributions

AUTHORS: Wilbur K. Brown[1], Lassen College, Susanville, CA 96130
Kenneth H. Wohletz, EES-1

PUBLISHED IN: Journal of Applied Physics
Vol.78, No. 4, 2758-2763, 15 August 1995,

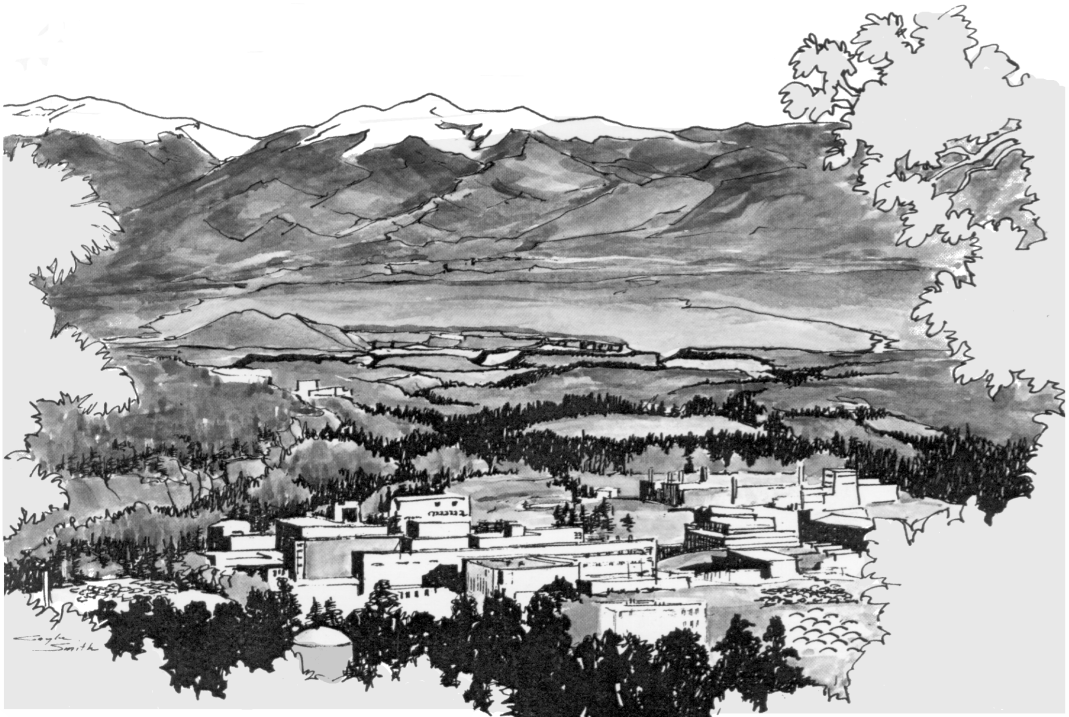

This is a preprint of a paper intended for publication in a journal or proceedings. Because changes may be made before publication, this preprint is made available with the understanding that it will not be cited or reproduced without the permission of the author.

Los Alamos
Los Alamos National Laboratory
Los Alamos, New Mexico 87545

[1]**Address for correspondence: 5179 Eastshore Drive, Lake Almanor, CA 96137 USA**

Derivation of the Weibull Distribution Based on Physical Principles and its Connection to the Rosin-Rammler and Lognormal Distributions

Wilbur K. Brown[a)]

Math/Science Division, Lassen College, Box 3000, Susanville, CA 96130

Kenneth H. Wohletz

Earth and Environmental Science Division, Los Alamos National Laboratory, Los Alamos, NM 87545

We describe a physically based derivation of the Weibull distribution with respect to fragmentation processes. In this approach we consider the result of a single-event fragmentation leading to a branching tree of cracks that show geometric scale invariance (fractal behavior). With this approach, because the Rosin-Rammler type distribution is just the integral form of the Weibull distribution, it, too, has a physical basis. In further consideration of mass distributions developed by fragmentation processes, we show that one particular mass distribution closely resembles the empirical lognormal distribution. This result suggests that the successful use of the lognormal distribution to describe fragmentation distributions may have been simply fortuitous.

I. Historical Background

In 1933 Rosin and Rammler[1,2] proposed the use of an empirical distribution for description of particle sizes, which they obtained from data describing the crushing of coal and other materials. In 1939 Weibull[3] proposed the same distribution (as we show below), which he obtained from the study of the fracture of materials under repetitive stress. The distribution proposed was strictly empirical[4], until Austin et al.[5] derived it to describe batch grinding in 1972. Later, Peterson et al.[6] and Brown[7], and Wohletz et al.[8] independently rederived the distribution. Austin et al., Peterson et al., and Brown each derived the distribution from a somewhat different point of view, but they all used a simple but nonetheless empirical power law to describe the breakup of a single particle into smaller particles. In this article we eliminate this shortcoming and thus put the Weibull distribution on a solid theoretical basis, stemming from physical principles.

II. Derivation of the Weibull Distribution

Brown[7] began his theory of sequential fragmentation with the equation

$$n(m) = C \int_m^\infty n(m')\, f(m' \to m)\, dm' \quad . \tag{1}$$

Here *n(m)* is the number distribution in units of particles per unit mass of mass *m* between *m* and *m + dm*. $f(m' \to m)$ is the single-event particle distribution function and expresses the distribution in mass, *m*, arising from the fragmentation of a single, more massive particle of mass m'. Equation (1) represents the summing of all contributions to the distribution of *m* from the fragmentation of all particles of mass $m' > m$.

Brown[7] set the constant *C* equal to m_1^{-1}, and chose

$$f(m' \to m) = \left(\frac{m}{m_1}\right)^\gamma \quad , \tag{2}$$

where $-1 < \gamma \leq 0$.

Inserting Equation (2) into Equation (1), we have

$$n(m) = \left(\frac{m}{m_1}\right)^{\gamma} \int_m^{\infty} n(m')\, d\left(\frac{m'}{m_1}\right) \quad . \tag{3}$$

The solution to Equation (3) is

$$n(m) = \frac{N_T}{m_1}\left(\frac{m}{m_1}\right)^{\gamma} \exp\left[-\frac{\left(m/m_1\right)^{\gamma+1}}{\gamma+1}\right] \quad , \tag{4}$$

which is the Weibull distribution in particle number. Equation (4) has been normalized such that

$$N_T = \int_0^{\infty} n(m)dm \quad , \tag{5}$$

where N_T is the total number of fragments in the distribution.

The cumulative form of Equation (4) is

$$\frac{N(>m)}{N_T} = \frac{\int_m^{\infty} n(m)dm}{\int_0^{\infty} n(m)dm} = \exp\left[-\frac{\left(m/m_1\right)^{\gamma+1}}{\gamma+1}\right] \quad . \tag{6}$$

Brown[7] defended his choice of Equation (2) on the basis of existing experimental data[9,10] (see, *e.g.*, Fig. 1 and refs. 9, 10) and the extensive successful empirical use of Equation (6). Until now, the use of Equation (2) was empirical, but as we shall see below, it has a deeper meaning based securely on physical principles.

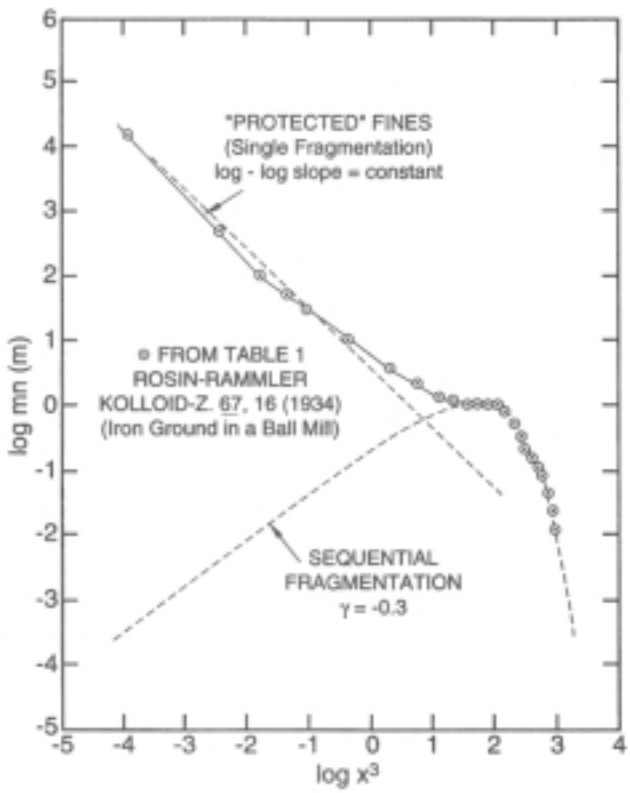

FIG. 1. Plot of log $mn(m)$ vs log x^3 where x is the particle diameter for iron ground in a ball mill (Rosin and Rammler, Ref. 17). Note that the data consist of two populations, fines that experienced a single fragmentation event and remained unaffected in spaces among larger particles that were repeatedly fragmented during milling.

The brittle fracturing of any particle results in a *branching tree of cracks* (Fig. 2), as discussed by Austin[11] and Van Cleef[12]. This branching tree of cracks looks the same on any scale, and thus can be described as a fractal[13]. As reiterated by Samson et al.[14], a method of describing such a thing as the fragments produced by a branching tree of cracks is the use of the *Covering Set* approach. Given a set of points in space, the following relationship holds true if the set is a fractal:

$$K(a) = a^{-D_f} \tag{7}$$

where *K(a)* is the number of segments (in one dimension) of length *a* needed to cover the set. Similarly, *K(a)* for a two- or three-dimensional set would correspond to the number of circles or spheres of radius *a*. In the present case, a set of spherical volumes describes the distribution of fragments resulting from the fractal cracking process, and D_f is the fractal dimension. For the

case where the fragmented material density is constant, the set of volumes becomes a set of masses. Equation (7) then becomes

$$f\,(m' \rightarrow m) = m^{-D_f/3} \tag{8}$$

where $\gamma = -D_f/3$, $-1 < \gamma \leq 0$, and $0 \leq D_f < 3$.

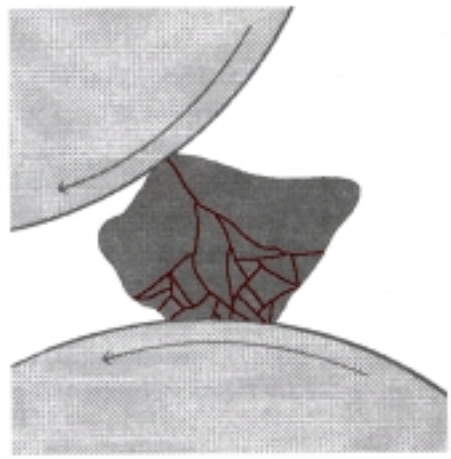

FIG. 2. Picture of tree of cracks after Austin (Ref. 11) and Van Cleef (Ref. 12) for a particle in a mill. The cracks observed during fragmentation are spaced in a manner that gives the fractal dimension, $D_f = -3\gamma$.

So in addition to the numerous meanings of the parameter γ discussed by Brown[7], we see that γ has a deeper meaning, namely that -3γ is the fractal dimension, D_f, which is generally understood to be a geometrically based attribute of a system[13]:

$$\gamma = -\lim_{m \to 0} \frac{\log f\,(m' \rightarrow m)}{\log\left(\frac{1}{m}\right)} = -\frac{D_f}{3} \tag{9}$$

Equation (2), then, has a solid basis in both theory and experiment, and the Weibull distribution is no longer empirical. We note that in writing this article, it is not our intention to investigate the phenomena involved in the actual cracking of material on a microscopic scale (*cf.* Grady[15]) nor do we pretend to be experts on the subject. We have chosen rather to investigate fragmentation of bulk matter and the resulting macroscopic mass distributions that, to our understanding, derive from far-field stresses as opposed to the near-field stresses that primarily determine particle surface textures.

III. The Connection with the Rosin-Rammler Distribution

The weight-size distribution proposed by Rosin and Rammler[1] in 1933 is

$$\frac{M(>\ell)}{M_T} = \exp\left[-\left(\frac{\ell}{\sigma}\right)^k\right] \quad . \tag{10}$$

Here, $M(>\ell)$ is the cumulative mass of all particles of mass greater than size ℓ, M_T is the total mass of the distribution, σ is a size related to the average size of the distribution, and the exponent k is a free parameter. Equation (10) has enjoyed extensive successful empirical use.

Equation (9) can be converted to a mass distribution by setting $\ell/\sigma = (m/m_2)^{1/3}$ so that

$$\frac{M(>m)}{M_T} = \exp\left[-\left(\frac{m}{m_2}\right)^{k/3}\right] \quad , \tag{11}$$

where m_2 is related to the average mass of the distribution.

Equation (10) is of the form of Equation (6) except that Equation (6) describes the cumulative <u>particle</u> distribution, whereas Equation (11) describes the cumulative <u>mass</u> distribution. Equation (6) is nevertheless of the Rosin-Rammler form.

If $n(m)$ describes the number of particles of mass m between m and $m+dm$ and each of the particles has mass m, then the mass distribution is just $mn(m)$, which is the total mass of particles of mass m between m and $m+dm$. The cumulative mass distribution is given by

$$M(<m) = \int_0^m mn(m)dm \quad . \tag{12}$$

Further,

$$\frac{dM}{dm} = mn(m) \quad . \tag{13}$$

By taking the derivative of Equation (11) with respect to m, we obtain

$$mn(m) = \frac{M_T}{m_2}\frac{k}{3}\left(\frac{m}{m_2}\right)^{k/3-1} \exp\left[-\left(\frac{m}{m_2}\right)^{k/3}\right] \quad . \tag{14}$$

This, too, is a Weibull distribution (the power on the left *(m/m₂)* is one less than the *(m/m₂)* in the square brackets), but Equation (14) is a Weibull distribution in <u>mass</u> whereas Equation (4) is a Weibull distribution in <u>particle number</u>. Another difference is that in Equation (4) the $f(m' \to m) = m^{\gamma}$ term now has a physical basis, whereas the corresponding term for Equation (11) does not[5]. We now see, however, that the derivative of any Rosin-Rammler distribution <u>is</u> a Weibull distribution. This observation indicates that the demonstrated physical basis for the Weibull distribution is true also for the Rosin-Rammler distribution.

IV. The Use of the Weibull Distribution

In his article Brown[7] advocated the use of the mass distribution, *mn(m)*, rather than the particle number distribution, *n(m)*, because the latter is tedious—if not impossible—to observe (the use of the cumulative distribution, Equation (6), has been preferred).

The mass distribution, *mn(m)*, from Equation (4) is

$$mn(m) = N_T\left(\frac{m}{m_1}\right)^{\gamma+1} \exp\left[-\frac{\left(m/m_1\right)^{\gamma+1}}{\gamma+1}\right] \quad . \tag{15}$$

Alternatively, if we make use of a logarithmic scale in m, say $u \equiv \ln m$, and note that

$$n(u)du = n(m)dm \quad , \tag{16}$$

then

$$mn(m) = n(u) \quad . \tag{17}$$

Thus *mn(m)* also gives the number of particles per unit natural logarithm in *m*.

Furthermore, if *mn(m)* is the number of particles per unit logarithm in m, and the mass of each particle is *m*, then the total mass of particles per unit logarithm is just $m^2 n(m)$. Thus

$$m^2 n(m) = N_T m_1 \left(\frac{m}{m_1}\right)^{\gamma+2} \exp\left[-\frac{\left(m/m_1\right)^{\gamma+1}}{\gamma+1}\right] \quad . \tag{18}$$

This distribution is shown in Figure 3 where it is compared to the lognormal distribution:

$$\lambda(m) = \frac{1}{\sigma\sqrt{2\pi}} \exp\left[-\frac{\left(\ln m - \ln m_3\right)^2}{2\sigma^2}\right] \quad , \tag{19}$$

where $\lambda(m)$ is the mass, m, distribution in units of mass per unit ln interval, m_3 is a constant that allows variable positioning of the curve, and σ is the standard deivation in ln m units.

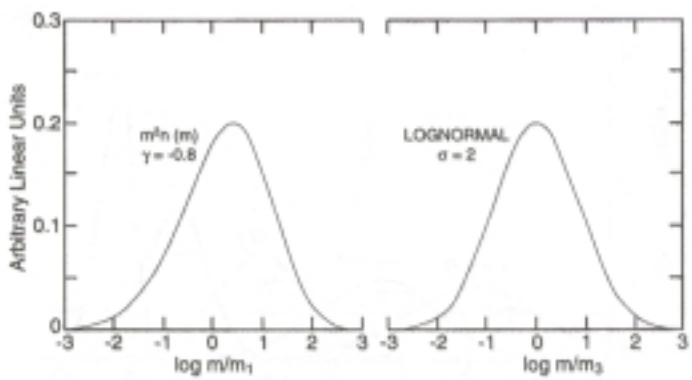

FIG. 3. Plot of $m^2 n(m)$ vs $\log m$ (where m_1 and m_3 are constants) compared to the lognormal distribution for $\gamma = -0.8$ and standard deviation $\sigma = 2$ ($\ln m$ units). Note the apparent similarity of the two distributions.

The quantity $m^2 n(m)$ is precisely what is measured when a sample of particles is sifted through a series of sieves of decreasing mesh size where the mesh sizes between any two adjacent sieves is a fixed ratio. As Brown and collaborators noted[7,8], the form $m^2 n(m)$ closely resembles the lognormal distribution[11] (see Fig. 3), a distribution that has enjoyed a long history of successful, empirical use; we note the lognormal distribution has a mathematical basis[16], but no physical basis.

The gathering of data through a series of sieves with a fixed size ratio between them is standard procedure in many fields; for example, in the analysis of geological materials such as

sand and volcanic ash. For this procedure, the mass left on each sieve ΔM, is recorded in a logarithmic bin of width $\Delta\phi$ where $\phi \equiv -log_2(\ell/\ell_0)$, and where $\ell_0 \equiv 1$ mm. It can easily be shown that

$$\frac{dM}{d\phi} = -3\ln 2 \;\; m^2 n(m) \quad . \tag{20}$$

The negative sign and the $\ln 2$ originate from the definition of the ϕ-scale, and the 3 provides the conversion from mass to size (assuming spherical particles of equal density). An illustration of the effect of varying γ in Equation (18) is shown by Figure 4 where distributions of different γ values are plotted as $dM/d\phi$ *vs* ϕ from Equation (20). This illustration shows that as γ increases (signifying that the particles are undergoing further processing), the distribution becomes finer in particle size and more *peaked*.

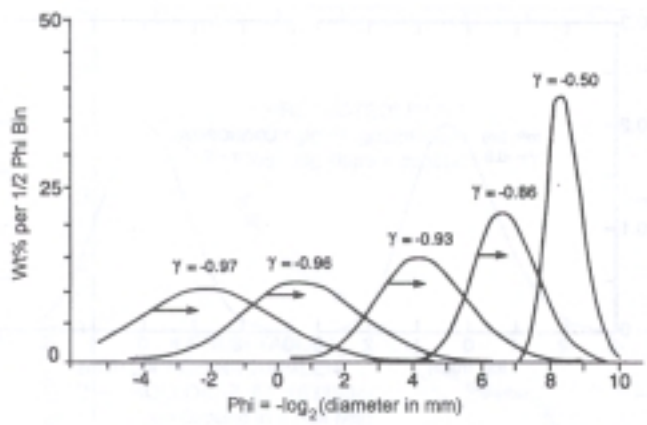

FIG. 4. Plot of $m^2 n(m)$ distributions in the form of $dM/d\phi$ vs ϕ, where $dM/d\phi$ is defined by Eq. (20), and $\phi = -\log_2$ (diameter in mm); the reader will recall that all log scales are proportional, and that the minus sign simply places the coarse particles to the left and the fine particles to the right. This plot shows the effect of varying γ in Eq. (18), where increasing γ shifts the peak of the distribution to the right (finer particle sizes) and makes the distribution more peaked. Note that where $\gamma = -1.0$ the distribution is flat.

As in many fields, the lognormal distribution has been typically used to describe the data because it is a convenient approximation to the shape of the data such as $dM/d\phi$. Although application of the lognormal distribution to this type of data is traditional, its satisfactory representation of the data may be simply fortuitous. In contrast, we believe that application of

Equation (18), giving $m^2n(m)$, is a more proper, physically based formulation to apply. An example of the use of $m^2n(m)$ for soot particle size data[18], using the mass to size conversion of Equation (20), is shown in Figure 5.

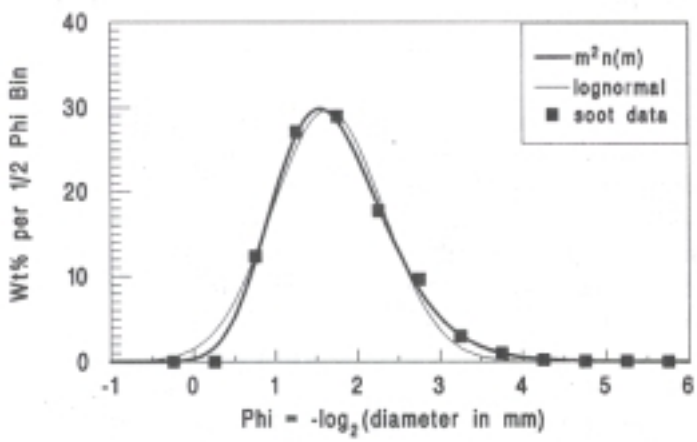

FIG. 5. An example of the use of $m^2n(m)$ for soot particle data from Medalia and Heckman (see Ref. 18). In this plot the $m^2n(m)$ curve crosses every data point but one, whereas the lognormal curve gives a less satisfactory fit. Each curve was best-fit to data by least-squares regression analysis; the $m^2n(m)$ curve explains 96% of the sample variance while the lognormal curve satisfies only 88%. As in Fig. 4, data and $m^2n(m)$ are expressed in distribution wt. % per 1/2 phi bins.

V. Characteristics of the Lognormal-Like $m^2n(m)$ Distribution

In general form, the equation describing $m^2n(m)$ is given by

$$m^2n(m) = N_T m_1 \left(\frac{m}{m_1} - \frac{m_0}{m_1}\right)^{\gamma+2} \exp\left[-\frac{\left(\frac{m}{m_1} - \frac{m_0}{m_1}\right)^{\gamma+1}}{\gamma+1}\right] , \tag{21}$$

where m_0 allows variable positioning of the distribution. The peak of the distribution, m_p (also called the most probable mass or the *mode*), may be obtained by taking the derivative of Equation (18) and setting the result equal to zero. We obtain

$$\frac{m_p}{m_1} = (\gamma+2)^{\frac{1}{\gamma+1}} \quad , \tag{22}$$

or

$$\log\frac{m_p}{m_1} = \frac{\ln(\gamma+2)}{(\gamma+1)\ln 10} \quad . \tag{23}$$

This function varies relatively slowly with γ.

We may find the average mass, $\overline{m}$, of the distribution by setting

$$\overline{m} = \frac{\int_{-\infty}^{\infty} m\left[m^2 n(m)\right] d\ln m}{\int_{-\infty}^{\infty}\left[m^2 n(m)\right] d\ln m} = \frac{\int_0^{\infty} m^2 n(m) dm}{\int_0^{\infty} m n(m) dm} \quad . \tag{24}$$

With the use of the complete gamma function

$$\Gamma(\alpha) = \int_0^{\infty} t^{\alpha-1} e^{-t} dt \quad , \tag{25}$$

we find that

$$\frac{\overline{m}}{m_1} = (\gamma+1)^{\frac{1}{\gamma+1}} \frac{\Gamma\left(\frac{\gamma+3}{\gamma+1}\right)}{\Gamma\left(\frac{\gamma+2}{\gamma+1}\right)} \quad . \tag{26}$$

Combining this result with m_p from Equation (22), we obtain

$$\frac{\overline{m}}{m_p} = \left(\frac{\gamma+1}{\gamma+2}\right)^{\frac{1}{\gamma+1}} \frac{\Gamma\left(\frac{\gamma+3}{\gamma+1}\right)}{\Gamma\left(\frac{\gamma+2}{\gamma+1}\right)} \quad . \tag{27}$$

The integrals involved in finding the standard deviation of $m^2 n(m)$ proved to be intractable. An approximate curve was found numerically for the full width at half maximum (*FWHM*). It is (in $\ln m$ units):

$$FWHM \approx \frac{2.3444}{\sqrt{\gamma+1}} - 0.68 - 0.17\ln(\gamma+1) \quad , \tag{28}$$

which is good to within <1% for the range of 0 < (γ+1) < 0.8 and to within 2% for 0.8 < (γ+1) <1.0. The data rarely (if ever) fall outside this range. At (γ+1) ➘ 0 the distribution is very broad and flat. At (γ+1) ≈ 1, the distribution is quite narrow and peaked. For the lognormal distribution, shown in Equation (19), $FWHM = \sigma\sqrt{2\ln 2}$. Figure 6 illustrates $\overline{m}$, m_p, and *FWHM* as described above.

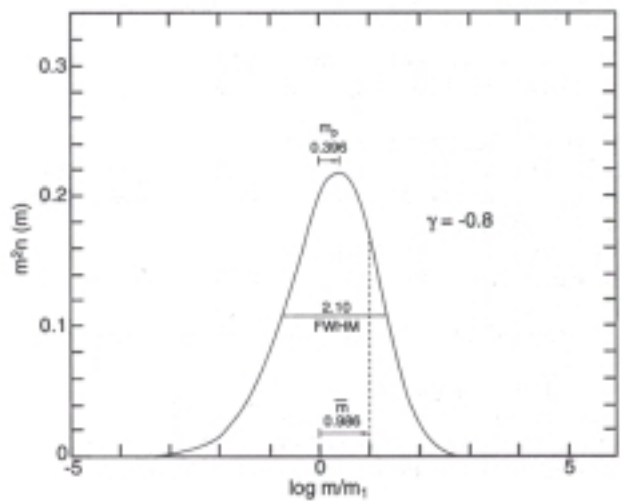

FIG. 6. Plot of $m^2n(m)$ vs $\log m/m_1$ for $\gamma = -0.8$, showing average particle mass $\bar{m}$, FWHM (full width and half maximum), and m_p, the particle mass at the distribution peak.

The cumulative mass of the distribution $m^2n(m)$ is obtained by setting

$$\frac{M(<m)}{M_T} = \frac{\int_{-\infty}^{\ln m} m^2 n(m)\, d\ln m}{\int_{-\infty}^{\infty} m^2 n(m)\, d\ln m} = \frac{\int_0^m m n(m) dm}{\int_0^\infty m n(m) dm} \quad . \tag{29}$$

The result is obtained with the use of the incomplete gamma functions

$$\Upsilon(\alpha, x) \equiv \int_0^x t^{\alpha-1} e^{-t} dt \quad , \tag{30}$$

and

$$\Gamma(\alpha, x) = \int_x^{\infty} t^{\alpha-1} e^{-t} dt \quad . \tag{31}$$

The results are

$$\frac{M(<m)}{M_T} = \frac{\Upsilon\left(\frac{\gamma+2}{\gamma+1}, x\right)}{\Gamma\left(\frac{\gamma+2}{\gamma+1}\right)} \quad , \tag{32}$$

and

$$\frac{M(>m)}{M_T} = \frac{\Gamma\left(\frac{\gamma+2}{\gamma+1}, x\right)}{\Gamma\left(\frac{\gamma+2}{\gamma+1}\right)} \quad , \tag{33}$$

where

$$x \equiv \frac{\left(m/m_1\right)^{\gamma+1}}{\gamma+1} \quad . \tag{34}$$

Figure 7 is a plot of $M(<m)/M_T$ *vs* $\log m/m_1$, whereas Figure 8 shows $\log m/m_1$ plotted *vs* $M(<m)$ in probability %.

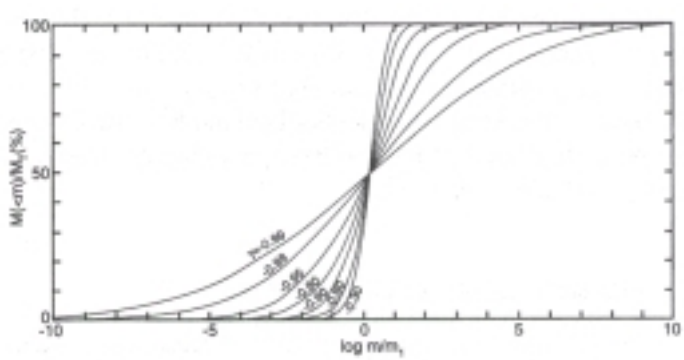

FIG. 7. Plot of $M(<m)/M_T$ vs $\log m/m_1$ for a range of γ values. The plot demonstrates that as γ becomes larger, the distribution becomes narrower.

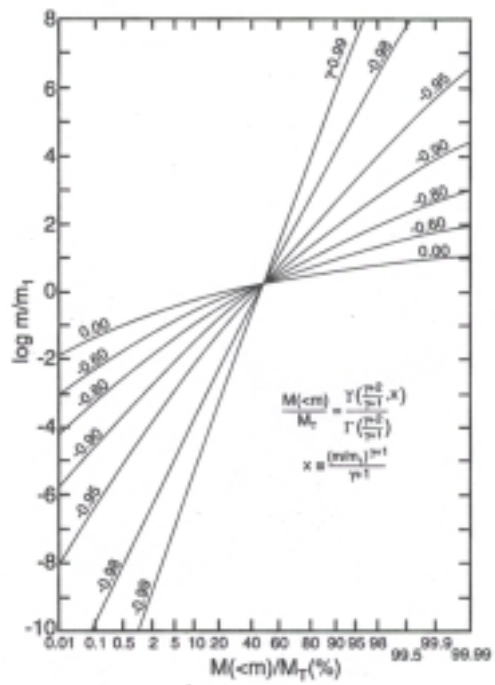

FIG. 8. Plot of $\log m/m_1$ vs $M(<m)/M_T$ in % probability. Note that as γ approaches -1, the curves become increasingly linear; a straight line would designate a lognormal distribution.

VI. Conclusions

Because the fragmentation of any single particle results in a branching tree of cracks that looks the same on any scale, the process can be described by a fractal. Further, the *Covering Set* approach leads to exactly the formulation previously and empirically used to describe the mass distribution of particles resulting from the fragmentation of a single larger particle. Thus all of the principal distributions used over the years to describe particle-sizes have a physical basis, and the fractal dimension, $D_f = -3\gamma$ ($0 \le D_f \le 3$), gives a deeper meaning to Brown's[7] parameter, γ, which is central to the problem of deriving the various distributions discussed.

In deriving the Weibull distribution from physical principles, we have shown that the Rosin-Rammler distribution is just the integral of the Weibull distribution so that it, too, has a physical basis. In our synthesis, we have defined the $m^2n(m)$ form of the mass distribution. This formulation closely resembles the lognormal distribution and suggests that the successful

empirical use of the lognormal distribution for particle size studies over the last century may have been simply fortuitous. This finding suggests that the same situation may exist in other fields where the lognormal shape has been empirically used, and has had legitimacy bestowed upon it by many years of use.

We thank an anonymous referee of this article for useful remarks.

References

[1]P. Rosin E. Rammler, J. Inst. Fuel **7**, 29 (1933).

[2] L. R. Kittleman, Jr., J. Sed. Petrol. **34**, 483 (1964).

[3]W. Weibull, The Royal Swedish Institute of Engineering Research (Ingenors Vetenskaps Akadiens Handlingar), Proc. No. **151**, Stockholm, (1939).

[4]W. Weibull, J. Appl. Mech. **18**, 293 (1951).

[5]L. G. Austin, P. T. Luckie, and R. R. Klimpel, Trans. Soc. Min. Engr. AIME **252**, 87 (1972).

[6]T. W. Peterson., M. V. Scotto, and A. F. Sarofim, Powder Tech. **45**, 87 (1985).

[7]W. K. Brown, J. Astrophys. Astr. **10**, 89 (1989).

[8]K. H. Wohletz, M. F. Sheridan, and W. K. Brown, J. Geophys. Res. **94**, 15,703 (1989).

[9]A. M. Gaudin, Trans. AIME **73**, 253 (1926).

[10]J. J. Gilvarry and B. H. Bergstrom, J. Appl. Phys. **32**, 400 (1961).

[11]L. G. Austin, In: *Handbook of Powder Science and Technology*, 562, (Van Nostrand Reinhold, New York 1984).

[12]J. Van Cleef, Am. Sci. **79**, 304 (1991).

[13]B. B. Mandelbrot, *The fractal geometry of nature*, (W. H. Freeman and Co., New York 1983).

[14]R. J. Samson, G. W. Mulholland, and J. W. Gentry, Langmuir **3**, 272 (1987).

[15]D. E. Grady, J. Geophys. Res. **86**, 1047-1054 (1981).

[16]D. McAlister, Proc. Roy. Soc. London **29**, 367 (1879).

[17]P. Rosin and E. Rammler, Kolloid-Z **67**, 16 (1934)

[18]A. I. Medalia and F. A. Heckman, Carbon **7**, 567 (1969)